Analysis of Upper-Nose Temper Embrittlement Phenomena in ASTM A533 Type B Class 1 Mn-Mo-Ni Pressure Vessel Steel

W. M. de VILLIERS, H. J. de KLERK
ISCOR Ltd., Pretoria, Republic of South Africa
C. A. SMAL
A. E. C. of S. A. Ltd., Pretoria, Republic of South Africa

ABSTRACT

Upper-nose temper embrittlement processes that occur during tempering of ASTM A533 Type B Class 1 low alloy steel is described. This embrittlement is related to microstructural phenomena, which include grain growth, carbide coarsening and sub-critical phase transformation. The effect of embrittlement on the mechanical properties is presented by means of time-temperature property diagrams.

1. INTRODUCTION

ASTM A533 Type B Class 1 Mn-Mo-Ni steel is utilised in critical applications such as pressure boundaries in primary loops of nuclear power plants. During manufacturing of such high integrity pressure vessels, tempering temperatures in the region of 595°C up to 675°C are regularly specified. The phenomenon where a decrease in toughness concurrent with the loss of strength during tempering in the temperature range above 600°C is known as upper-nose temper embrittlement (UNTE). In literature the phenomenon is attributed to mainly carbide growth phenomena. The rate of embrittlement is shown to coincide with the softening kinetics of tempering (Martin et al. 1962; Naylor et al. 1981). The effect of grain growth on the toughness properties have not previously been shown to be important in Mo-containing low alloy steel types. The effects of sub-Ac_1 ferrite-austenite phase transformation have also not received adequate attention in literature.

2. EXPERIMENTAL

A 41mm thick plate sample of from an experimental production cast of ASTM A533 Type B Class 1 material was obtained in the as-quenched condition. The quenching was done by continuous roller quenching after austenitising at 910°C for 74 minutes, yielding a lower bainite microstructure. The chemical analysis of the plate sample is given in Table 1. Samples of 180mm x 150mm were exposed to tempering treatments in a forced air circulation laboratory furnace at temperatures of 630°C, 660°C, 675°C, 690°C, 705°C and 720°C, for exposure periods of 1h, 5h, 25h and 125h. The temperature in the furnace was controlled to within 2°C of the set point.

Charpy V-notch (CVN) coupons were prepared from each of the samples described above, and tested at various temperatures in the transition temperature range. Measurements of the impact energy were made from which the 68J ductile-brittle transition temperature (DBTT) was determined by means of interpolation of the average energy values. Tensile coupons were prepared from each of the heat treated samples and tested at room temperature. The proof strength value was taken at a proportional strain of 0,2% ($\sigma_{0,2}$).

Thin foils for transmission electron microscopy (TEM) were prepared from rods machined from selected fractured CVN coupons from each of the heat treated samples. Discs were sectioned from these rods and thinned by means of grinding and twin jet electro-polishing. The thin foils were studied in a JEOL 200CX STEM unit using the bright field mode at 200 kV accelerating voltage.

TABLE 1: Chemical analysis of the plate sample.

%C	%Mn	%P	%S	%Si	%Ni	%Mo	%Cr	%Cu	%Al
0,15	1,40	0,012	0,003	0,26	0,52	0,53	0,02	0,01	0,030

3. RESULTS AND DISCUSSION

3.1 Mechanical properties

Figs. 1 and 2 give the trends of 0,2% proof strength ($\sigma_{0,2}$), and ductile-brittle transition temperature (DBTT) as a function of tempering temperature.

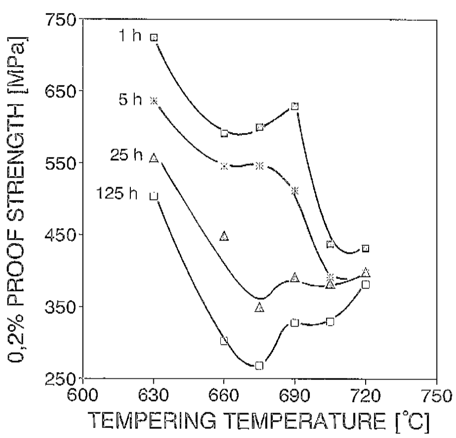

Fig. 1: 0,2% Proof strength ($\sigma_{0,2}$) as a function of tempering temperature.

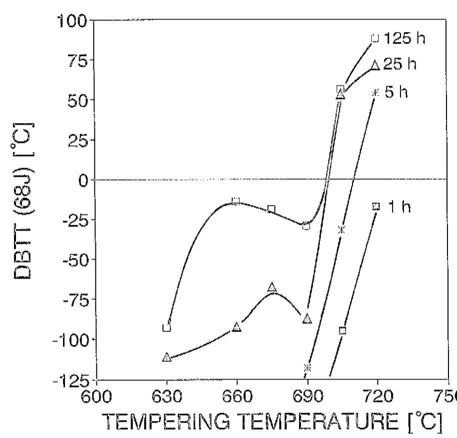

Fig. 2: The 68J DBTT as a function of tempering temperature.

3.2 Microstructural processes

In literature, tempering at high temperatures involves four different time-dependent microstructural changes, which have an effect on the DBTT, namely

i) a decrease of the dislocation density of the matrix

ii) a decrease of the carbide-precipitate density in the matrix

iii) recrystallisation and grain growth of the matrix structure

iv) dissolution of the matrix carbides and the formation of coarse grain boundary carbides (Pienaar 1986)

The present study portrays the important embrittling effect of grain growth phenomena and the deleterious effect of the formation of a dual phase microstructure on the toughness of a lower bainite original microstructure.

Fig. 3 shows a typical grain boundary region equilibrium carbide similar to those reported in literature (Pienaar 1986). Evidence of recrystallisation and grain growth phenomena was observed in most of the samples that were tempered

Fig. 3: Coarse carbide (κ) that formed on a prior austenite grain boundary during tempering at 660°C for 125h. α = ferrite

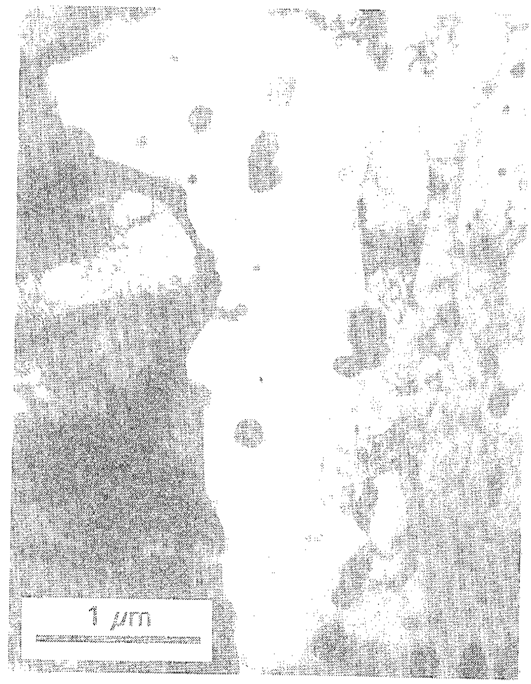

Fig. 4: Evidence of the formation of a new grain in the region of a prior austenite grain boundary during tempering at 660°C for 1h.

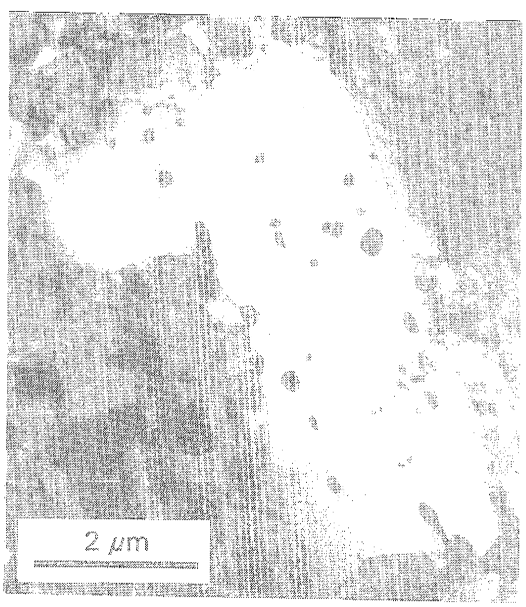

Fig. 5: A ferrite grain that is the result of recrystallisation and possibly grain coarsening reactions after tempering at 675°C for 5h.

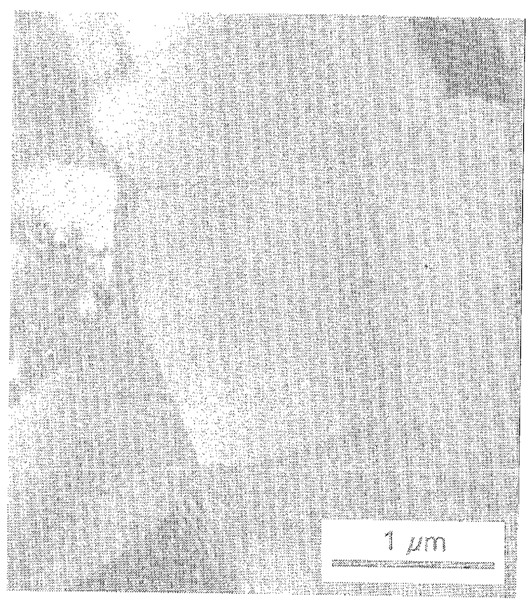

Fig. 6: Polygonisation of the ferrite matrix after tempering at 660°C for 25h.

in the 630°C-705°C temperature range. Figs. 4 to 6 show features that are the result of recrystallisation and grain coarsening. Fig. 4 shows the formation of a new grain in the region of a prior austenite grain boundary. Fig. 5 shows a similar ferrite grain after more heavy tempering. Fig. 6 shows the polygonised microstructure that results after heavy tempering; the various grains are "divided" by mostly low angle grain boundaries.

Evidence of the formation of metastable austenite below the usually accepted ferrite-austenite transformation temperature is shown in Fig.7. Pistorius et al. (1991) observed a definite deviation from linearity at temperatures even lower than 600°C, using a sensitive dilatometry technique, indicating the onset of ferrite-austenite phase transformation. It must be stated however, that significant amounts of fresh martensite and austenite was observed in samples treated at temperatures of 690°C and higher only. An example of the dual phase microstructure that is associated with very poor toughness is shown in Fig. 8. The extent of the embrittlement associated with the formation of austenite/martensite at temperatures above 690°C is illustrated in Fig. 2. These results are in contrast with the work of Forch et al.(1985) who found an improvement in toughness when a ferrite+upper-bainite microstructure is intercritically heat treated for long periods. Their results were obtained on an upper-bainite microstructure which exhibited an increase in toughness through a grain refining effect of the dual phase microstructure.

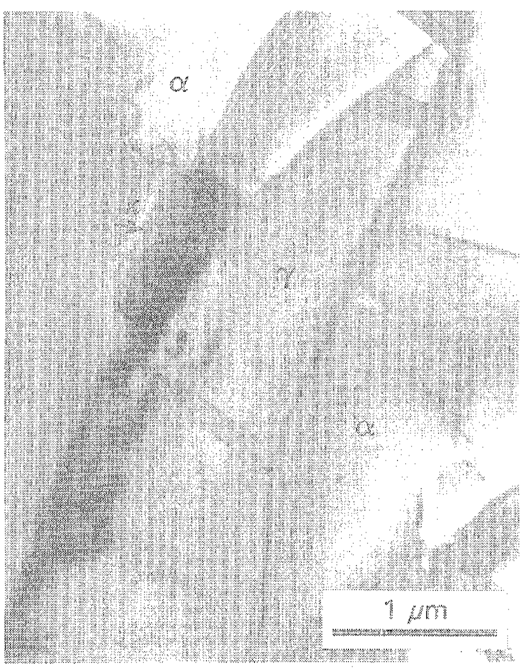

Fig 7: A metastable austenite island (γ) and equilibrium carbide (κ) that formed during tempering at 690°C for 125h. α = ferrite

Fig 8: Dual phase ferrite (α) - martensite (m) microstructure that resulted from tempering at 720°C for 125h.

3.3 Structure-property relationships

The effect of microstructural phenomena on toughness, and therefore also the degree of embrittlement, can conveniently be explained in terms of its relative effects on the proof strength and the cleavage fracture strength of the steel.

The usual form of the Hall-Petch equation (Petch 1986) for the yield strength σ_y, as a function of microstructural parameters, is as follows:

$$\sigma_y = \sigma_i + k_y d^{-1/2} \tag{1}$$

where σ_i is the base strength of the ferrite matrix, k_y the dislocation locking factor and d the ferrite grain diameter.

The cleavage fracture stress σ_{cleave}, of a ferritic steel, was shown by Petch (1986) to be as follows:

$$\sigma_{cleave} = \left[\frac{8\,\mu\,\gamma_p}{\pi(1-\nu)t} - \frac{k_y^2\,d}{8\pi^2 t^2}\right]^{1/2} - \frac{k_y\,d^{1/2}}{2\sqrt{2}\;\pi t} \tag{2}$$

where t is the grain boundary carbide thickness, μ the rigidity modulus, γ_p the effective surface energy appropriate for the passage of a crack from carbide to ferrite and ν Poisson's ratio. The microstructure that is presently under investigation is tempered bainite, indicating that an adjustment to Equation (2) is possibly required.

Through Equation (1), the effect of UNTE on the yield strength in the temperature range 630°C-690°C can be understood in terms of an increase in grain size, d, and a decrease in the magnitude of the resistance to dislocation movement in the ferrite matrix, σ_i. In the temperature range above 690°C austenitisation limits grain growth while martensite formation increases the dislocation density and thus σ_i.

In the temperature range 630°C-675°C, the embrittlement can be understood in terms of an increase in the thickness of the grain boundary carbides, t, and an increase in the grain size, d (Equation (2)). At 690°C a significant amount of austenite forms. Austenitisation restricts ferrite grain growth with a resultant slight increase in toughness. At temperatures above 690°C, large grain boundary carbides and the presence of an increased fraction of "fresh" martensite on cooling result in severe embrittlement. This strong effect of the dual phase microstructure can be partly explained by the effect of martensite on the mechanism of cleavage initiation and an increase in the local dislocation locking factor (k_y).

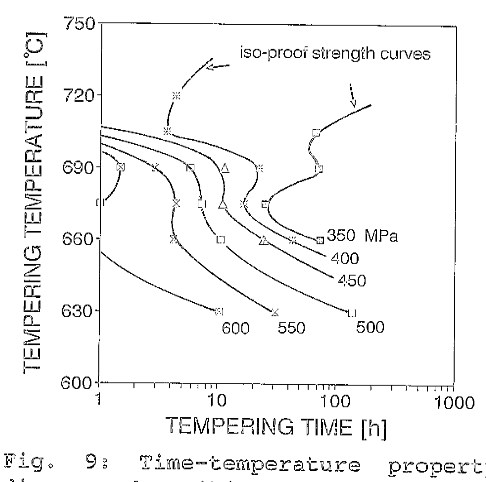

Fig. 9: Time-temperature property diagram describing the effect of tempering on $\sigma_{0,2}$.

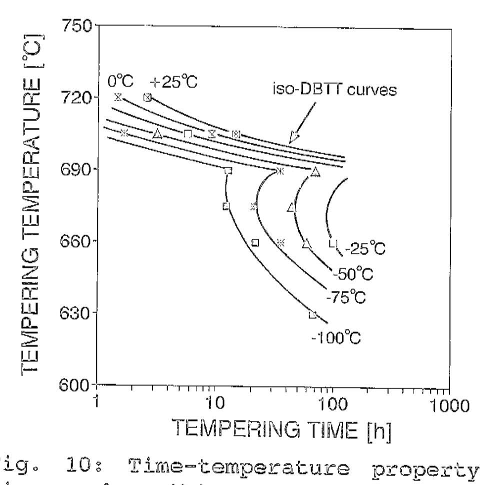

Fig. 10: Time-temperature property diagram describing the effect of the UNTE on DBTT (68J).

3.4 Time-temperature-property diagrams

Fig. 9 portrays the tempering behaviour in terms of $\sigma_{0,2}$ as a function of exposure (time and temperature), while Fig. 10 shows DBTT in terms of tempering temperature and exposure period. These figures provide a method to present the mechanical properties so that the effect of the microstructural development is clear. In Fig. 10, for the temperature range 630°C to 690°C, the embrittlement is mainly attributable to grain growth and carbide growth. The severe embrittlement in the temperature region from 690°C to 720°C is associated with the formation of a dual phase microstructure. These diagrams can be utilised as a design tool and during manufacturing to assess the effects of tempering treatments.

4. CONCLUSIONS

The mechanism of UNTE in Mn-Mo-Ni pressure vessel steels can be described in terms of six microstructural processes, namely
- a decrease of the dislocation density of the matrix,
- a decrease of the carbide-precipitate density in the matrix,
- recrystallisation and grain growth of the matrix structure,
- the formation of coarse grain boundary carbides,
- abnormal grain growth, and
- sub-critical ferrite-austenite phase transformation that results in a dual phase microstructure that consists of islands of metastable austenite and fresh martensite in ferrite.

The occurrence of the various embrittlement mechanisms is associated with particular temperature ranges:
- carbide coarsening in the temperature range 630° to 705°C,
- grain growth and coarsening in the temperature range 630° to 705°C,
- austenitisation processes in the temperature range 675° to 720°C, and
- interaction between carbide growth, grain growth and austenitisation processes in the temperature range 675° to 705°C.

ACKNOWLEDGEMENT
This work is published with the support of ISCOR Ltd.

REFERENCES

Forch,K., Piehl,K-H., Witte,W. (1985). Effect of the Precipitation Condition of the Carbide Phases on the Toughness Properties of Heavy Forgings from steel Grade 20MnMoNi 5. Thyssen Technische Berichte, Vol. 1/85: pp.34-41.

Martin,P.F., Roques,C., Bastien,P. (1962). Étude de la Fragilisation D'Aciers Soudables au Manganèse-Molybdène au Cours des Revenus de Détente Après Soudage. Revue de Métallurgie, Vol. 59: pp.829-843.

Naylor,J.P., Guttmann,M. (1981). Mechanism of Upper-nose Temper Embrittlement in Mn-Ni-Mo A533 gr.B Steel. Metal Science, Vol. 15: pp.433-441.

Petch,N.J., (1986). The Influence of Grain Boundary Carbide and Grain Size on the Cleavage Strength and Impact Transition Temperature of Steel. Acta metallurgica, Vol. 34: pp.1387-1393.

Pienaar,G., (1986). Effects of Vanadium on Upper-nose Temper Embrittlement and other Mechanical Properties of Cr-Ni-Mo Low Alloy Steels. Materials Science and Technology, Vol. 2: pp.1051-1061.

Pistorius,P.G.H., Van Rooyen,G.T., (1991). Article submitted to Acta metallurgica et materialia.